Desalination and Water Treatment
www.deswater.com
doi: 10.5004/dwt.2020.26181

202 (2020) 95–104
October

Optimizing induced struvite crystallization in a fluidized bed reactor for low-strength ammonium wastewater treatment

Jingyao Wang, Hui Gong*, Xiang Liu, Zhimou Wei, Kaijun Wang*

State Key Joint Laboratory of Environment Simulation and Pollution Control, School of Environment, Tsinghua University, Beijing 100084, China, emails: gongh14@tsinghua.org.cn (H. Gong), wkj@tsinghua.edu.cn (K. Wang), yaowanttofly@163.com (J. Wang), gclx_2007@126.com (X. Liu), ayweizhimou@sina.com (Z. Wei)

Received 31 August 2019; Accepted 27 May 2020

ABSTRACT

Struvite crystallization for low-concentration ammonium wastewater provides a promising yet challenging way to recover nitrogen from bulk municipal wastewater. This research focused on the direct removal of low-concentration NH_4^+–N by fluidized bed reactor (FBR) with induced crystallization. NH_4^+–N (30 mg/L) was efficiently removed and Mg^{2+} and PO_4^{3-} were employed as the precipitation reagents. The maximum of 82.0% NH_4^+ was removed when the pH was 10 and the stoichiometric ratio of $[NH_4^+]$:$[PO_4^{3-}]$:$[Mg^{2+}]$ was 1:1.1:1. The rank of the influences of the three single factors on NH_4^+–N removal efficiency (%) was pH > P:N > Mg:N. The crystals achieved under optimal conditions were mainly struvite, while the addition of excess phosphate (N:P = 1:1.5) promoted the formation of crystals clusters instead of maintaining the typical orthorhombic structure, until $Mg_3(PO_4)_2{\cdot}22H_2O$ formed with an N:P ratio of 1:1.625. As most previous studies mainly focused on high-strength wastewater, this research demonstrated the potential of induced struvite crystallization by FBR for nitrogen recovery from low-strength ammonium wastewater treatment.

Keywords: Struvite; Induced crystallization; Nitrogen recovery; Low-strength ammonia; Fluidized bed reactor

1. Introduction

Low-strength ammonium (NH_4^+–N) wastewater, such as sewage, was one of the main sources of nitrogen pollution which led to severe waterbody eutrophication. Excess accumulation of NH_4^+–N also undermined the nitrogen balance of the global ecosystem, decreased dissolved oxygen levels, and was toxic to aquatic organisms [1], all of which led to ever-stricter discharge limits for wastewater treatment plants [2]. The tougher discharge regulations undoubtedly placed a greater energy and chemical consumption burden on wastewater treatment plants with regard to nitrogen removal, which was mainly achieved using biological processes [3] to convert ammonia into nitrogen gas. However, because the Haber–Bosch process consumes a great deal of energy and nearly half of the commercialized hydrogen gas worldwide is used for ammonia production, recovering ammonium rather than destroying it seems to be a reasonable goal and should be carefully considered for wastewater treatment. Recently, the idea of recovering ammonium from low-strength wastewater was investigated [4–7]. Logan [8] calculated that 30 mg/L ammonia (the initial mainstream concentration was 20–75 mg/L for municipal wastewater) was equivalent to 0.25 kWh/m^3, which was nearly half the energy used for conventional wastewater treatment, and proposed ending ammonia addiction to fossil fuels by considering recovering low-strength nitrogen and also green energy such as solar for hydrogen production.

Struvite crystallization was one of the most widely used technologies for nitrogen/phosphorus recovery, which could

* Corresponding authors.

simultaneously remove and recover phosphorus (P) and nitrogen (N) from wastewater [9,10]. Struvite (also called magnesium ammonium phosphate or MAP) can be used as a fertilizer with a low leaching rate [11] to provide nutrients during the plant-growing season or as a binding material in cement [12]. It was reported that insoluble struvite was easily separated from the water phase as a soft mineral with a low specific gravity which would not be flushed away by rainfall, thereby making it suitable for application even in flooded areas, as opposed to highly soluble fertilizers, which are undesirable [13]. Previous literature reported nutrient recovery by struvite from human urine [14], calf manure [15], leather tanning wastewater, swine wastewater [16], waste sludge anaerobic digestion rejected water [17], sludge dewatering liquor [18], industrial wastewater, municipal landfill leachate, and poultry manure wastewater [19]. The precipitation of struvite was affected by several factors including pH, concentrations of Mg^{2+}, PO_4^{3-}, and NH_4^+, and the presence of other interfering ions, such as calcium (Ca^{2+}) [20]. It was also highly pH-dependent, as activities of both NH_4^+ and PO_4^{3-} were affected by solution pH [16]. However, most previous research focused on struvite crystallization for high-strength ammonia wastewater rather than low-strength wastewater (such as sewage), which was more challenging with quite different solution conditions and required comprehensive investigation [21].

Reactor configuration was also crucial for nutrient recovery by struvite. Due to the difficulties of struvite fines for their retainment in reactors, which led to lower recovery efficiency and poorer effluent quality, induced struvite crystallization in the fluidized bed reactor (FBR) has drawn a great deal of attention [22]. Heterogeneous nucleation during induced crystallization promoted struvite crystal growth based on feeding embryo (such as silica sands and recycled small struvite crystals). Induced crystallization also changed the metastable zone and reduced the chemical consumption for low-concentration crystallization. In Song et al. [23], a sequencing batch reactor and a continuous flow reactor, both of which had struvite accumulation devices, were designed and used in a pilot plant and stainless steel mesh was used as an inducer and carrier to recover N (410–1,379 mg/L) and P (22.2–68.7 mg/L) from anaerobically digested swine wastewater. This was carried out by struvite crystallization without chemical additions. Prywer and Torzewska [24] used *Proteus* bacteria to induce struvite crystallization from synthetic urine and found that the crystal growth was theoretically related to the bacterial substances which served as the sites for heterogeneous nucleation. Besides struvite, induced crystallization in FBR was also proposed for other precipitation for the recovery of heavy metals such as copper [25]. If efficient induced crystallization for low-strength ammonia wastewater could be widely achieved, it was expected that the global nitrogen cycle could be improved with a lower energy burden and a more efficient application of materials [26]. However, as mentioned above, most previous research paid more attention to high-strength wastewater than to low-strength wastewater. To our best knowledge, no studies on the direct removal of low-concentration ammonia from municipal wastewater by FBR-induced crystallization have been reported.

In this study, an FBR for struvite crystallization was constructed to evaluate its applicability for low-strength ammonium wastewater. Factors impacting induced crystallization were comprehensively investigated including recirculation flux, pH, and a molar ratio of $[Mg^{2+}]$:$[NH_4^+]$:$[PO_4^{3-}]$, which was also optimized using the response surface methodology (RSM) method. The characteristics of the struvite crystals that were obtained, including their structure and composition and the surface morphology of the solid precipitates, were also analyzed via X-ray diffraction (XRD) and scanning electron microscopy (SEM).

2. Materials and methods

2.1. Chemicals

All of the reagents, including $MgSO_4{\cdot}7H_2O$, NH_4Cl, and $NaH_2PO_4{\cdot}2H_2O$, used in this study were analytical chemicals (Sinopharm Chemical Reagent Co., Ltd., China). All of the solutions were prepared with distilled water (Table 1). The pH was adjusted by sodium hydroxide and hydrochloric acid solution. Silica sands with an average diameter of 0.18 mm after sifter screening were used as seed grains for induced crystallization. $NaH_2PO_4{\cdot}2H_2O$ was added to 30 mg/L NH_4^+–N solution (25 L) to obtain various molar ratios of $[NH_4^+]$:$[PO_4^{3-}]$ under adjusted pH.

2.2. FBR setup

All of the experiments were performed at room temperature using a laboratory-scale FBR (Fig. 1). The FBR was composed of a Plexiglas column with an inner diameter of 3 cm and a height of 50 cm. A settling zone was set on top of the reactor. The FBR was filled with silica sands, which were cleaned by 15% of nitric acid before use. The static height of the sand bed in the reactor was 20 cm. The synthetic wastewater and precipitant were injected into the reactor from the sides at the bottom by a peristaltic pump. The circulation reflux was fed constantly from the bottom of the reactor at a given flow rate to fluidize the sands. The circulation reflux was set as 100, 150, and 200 mL/min by a peristaltic pump. All experiments in this investigation were operated at a flow of 16.67 mL/min and a hydraulic retention time of 1 h. Struvite ($MgNH_4PO_4{\cdot}6H_2O$) was sparingly soluble under neutral and alkaline conditions but readily soluble in acid and was produced under alkaline conditions [27]. Burns and Finlayson [28] have suggested that the minimum pH of the solution should be 7 to obtain favorable struvite precipitation. So, batch experiments were performed under alkaline conditions in this research.

2.3. Hill-climbing (single factor) experiment of NH_4^+–N removal efficiency

The single factor experiment was carried out by selecting four factors in the process: recirculation flux, pH, P:N, and Mg:N. Different gradients were set respectively (recirculation flux was 100, 150, and 200 mL/min; pH was 8, 9, 10, and 11; P:N was 0.8, 1, 1.1, 1.2, 1.5 and 1.8; Mg:N was 0.7, 0.8, 1, 1.2 and 1.5), and the optimal single factor level was selected by measuring the NH_4^+–N removal efficiency in the process.

Table 1
Formulation of the synthetic wastewater

Chemicals	Mother liquid concentration (mg/L)
$MgSO_4 \cdot 7H_2O$	51.4 (Mg)
NH_4Cl	30.0 (N)
$NaH_2PO_4 \cdot 2H_2O$	66.4 (P)

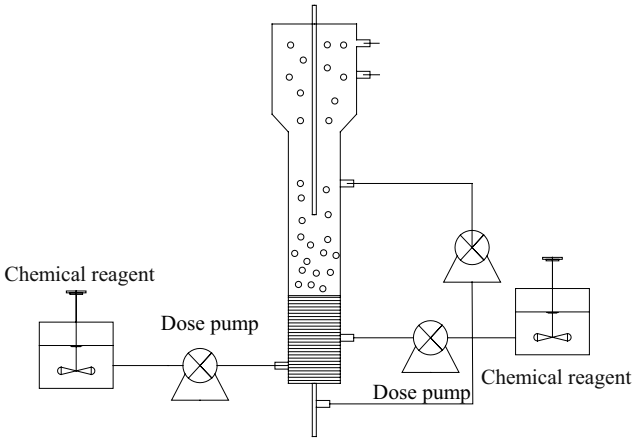

Fig. 1. Schematic diagram of the fluidized bed reactor (FBR) used in this study.

2.4. Optimization of NH_4^+–N removal using RSM

Base on the data of the hill-climbing experiment, RSM with central composite design (CCD) was used for optimization experiments. A total of 20 experimental runs with combinations of pH, P:N, and Mg:N were conducted. A CCD with three levels for all three factors was used for this purpose (Table 2). The CCD, which provided equally good predictions at points equally distant from the center, consisted of 2*k* factorial runs with *k* axial runs and *n* 0 center runs, where *k* stands for the number of factors. In this study, as the Table 2 shown, pH, *n*(N):*n*(P), and *n*(N):*n*(Mg) were chosen as factors X_1, X_2, and X_3, and the response was NH_4^+–N removal efficiency.

2.5. Analysis methods

Effluent samples were collected every 2 h using a disposable syringe. NH_4^+ and PO_4^{3-} were analyzed by spectrophotometry and filtered using a 0.22 μm membrane before measurement. The concentration of ammonia nitrogen was measured by Nessler Method using a UV-Spectrophotometer (UNICO 2800A, China) with the wavelength set at 420 nm. The amount of phosphate was determined by the molybdovanadate method using a UV-Spectrophotometer (UNICO 2800A, China) with the wavelength set at 700 nm. Morphological and microstructural observation of the deposits on the sand grains was performed by SEM (Philips XL 20). The crystal structure of the precipitate was analyzed by XRD (Rigaku D/Max-2500) in a dried state. The saturation index, defined as log IAP-logK_s, represented oversaturation as a positive value and undersaturation as a negative value, where IAP was the ion activity product and K_s was the solubility product.

Table 2
Response surface analysis of factors and levels

Factor	Code	Level		
		−1	0	+1
pH	X_1	9	10	11
P:N	X_2	0.8	1.1	1.4
Mg:N	X_3	0.8	1	1.2

3. Results and discussion

3.1. Induced crystallization promoted struvite precipitation in low concentrations

Synthetic wastewater was used to evaluate induced struvite crystallization to recover ammonium from low-strength municipal wastewater. Recently, paradigm-shifting for municipal wastewater was proposed to use "organic pre-concentration + mainstream anammox" to replace traditional activated sludge process. During organic pre-concentration, organics, which could be used for energy generation by following anaerobic digestion, could be separated from mainstream wastewater by various methods including A-stage, high rate contact stabilization, and membrane technology. The remaining nitrogen in the mainstream was proposed to be removed as nitrogen gas by an anammox process, which was autotrophic and low energy consumption. However, the R&D of mainstream anammox was still in progress. This research discussed another option that after organic pre-concentration, the remaining nitrogen was recovered as resources instead of being removed as nitrogen gas. Since most organics even suspend solid could be removed during the organic pre-concentration stage, synthetic wastewater was used to simulate wastewater in this condition.

Crystal growth was affected by surface diffusion, degree of solution supersaturation, and mass transfer efficiency [29]. Theoretically, struvite crystallization was more difficult with low-concentration ammonia. The supersaturated system in the metastable zone remained stable without the interference of external conditions. As shown in Fig. 2a, when the N:P:Mg = 1:1:1, no precipitation was observed in the beaker. However, in the fluidized bed crystallization reactor, the limitation of mass transfer was reduced by improved turbulence degree, which led to increased crystal growth, as shown in Fig. 2b. In general, as shown in Fig. 2c, the solubility curve and the supersaturation curve of the solution divided the supersaturated solution into three regions: the stable region, the metastable region, and the unstable region [30]. When the feeding carrier was added into the solution or there was external flow disturbance, the solute took the carrier as the embryo for crystal growth. The solute concentration point gradually decreased to the solubility curve, indicating that struvite precipitation began as induced crystallization [31].

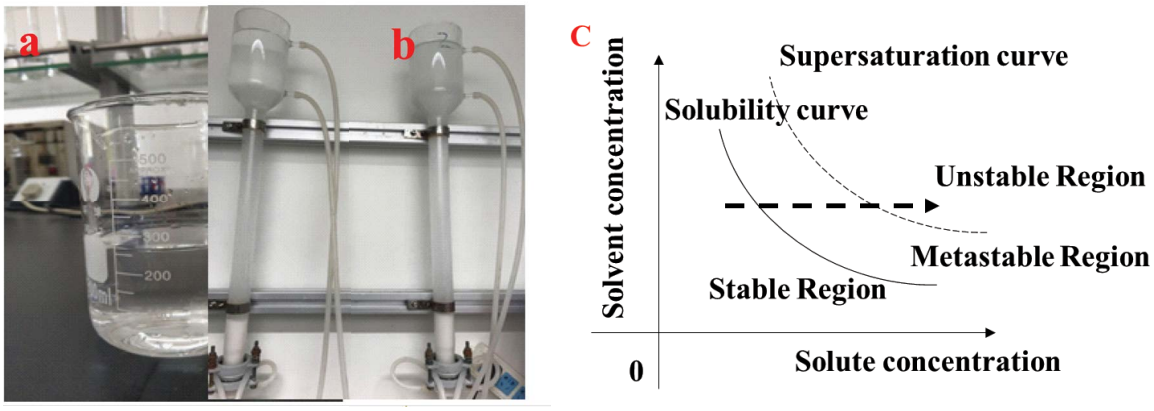

Fig. 2. Process of struvite formation in FBR with beaker as control. (a) No precipitation in beaker, (b) struvite in FBR at idle state, and (c) solubility zone, super solubility zone, and metastable zone during induced crystallization.

3.2. Optimization for induced struvite precipitation

3.2.1. Effects of recirculation flux, pH, N:P, and N:Mg on nitrogen removal

As shown in Fig. 3a, as the recirculation flux velocity decreased, the removal efficiency of NH_4^+ increased, though longer contact time was beneficial to removal efficiency, demonstrating that precipitation kinetics could play a more important role [13]. However, because in actual operation a recirculation flux of less than 100 mL/min caused precipitation in reactor and pipe joints, a minimum recirculation flux of 100 mL/min was chosen in this study.

The changes in ammonia nitrogen removal efficiency with pH are shown in Fig. 3b. The existing status and the concentrations of three participating ions depend directly on the pH value of the solution [32]. The crystallization of struvite occurred when the IAP of Mg^{2+}, NH_4^+, and PO_4^{3-} exceeded its solubility product (K_{SP}) [33]. The pH value appeared to be the critical factor that affected ammonium concentration since a slight rise in pH caused a significant decrease in ammonium content at a fixed molar ratio of either Mg/N or P/N [12]. At pH 8–10, the NH_4^+ removal efficiency increased along with the pH and progressively reached a peak at pH 10. Struvite formation reaction was a reversible process [12]. When the pH was under 8, the high content of H^+ in solution inhibited the struvite crystallization process, resulting in low removal efficiency. As the pH increased from 8 to 10, the decrease of H^+ concentration facilitated an increase in the HPO_4^{2-} concentration [34]. This promoted struvite formation, resulting in a rapid increase of ammonia nitrogen removal. Further increasing the pH over 10 caused a significant decrease in nitrogen removal. This was primarily because at pH > 10 the majority specie of ammonia nitrogen in solution was converted from NH_4^+ to NH_3, which could not be used for struvite crystallization.

It was reported that supersaturation plays a major role in struvite formation [35]. Theoretically, the molar ratio of Mg, N, and P in struvite was 1:1:1 [36]. In actual reactions, however, MAP ($MgNH_4PO_4$) formed a hard crystalline deposit when the molar ratio of Mg:N:P was greater than 1:1:1 [37]. From Fig. 3c, it was observed that as the N:P molar ratio increased from 1:0.8 to 1:1.1, the ammonia nitrogen removal efficiency progressively increased to a maximum (82%) at N:P of 1:1.1. Yetilmezsoy and Sapci-Zengin [28] also reported that reduction in molar ratios of magnesium and phosphorus negatively affected NH_4–N removal. Uysal et al. [37] revealed that the removal efficiency of NH_4–N was 88.79% when the Mg:N:P molar ratio was 1:1:1, but that it decreased significantly to 54.39% when the ratio was 1:1:0.5. It was also stated by Ryu et al. [38] that the amount of added PO_4–P significantly affected NH_4–N removal and that an overdose of PO_4^{3-} increased the supersaturation degree for better struvite crystallization [39]. When the N:P ratio exceeded 1:1.1, ammonia nitrogen removal efficiency decreased. It should be noted that the residual PO_4^{3-} concentration in the supernatant began to rise as shown in Fig. 3c. This was caused by exhaustion of Mg^{2+} and NH_4^+ when the N:P was greater than 1:1.1. Thus, rather than increasing ammonia nitrogen removal efficiency, an overdose of PO_4^{3-} caused residual PO_4^{3-} in solution.

Adjustment of the Mg^{2+} concentration was another important measurement for controlling MAP crystallization. As shown in Fig. 3d, as the N:Mg ratio increased, the removal efficiency of NH_4^+–N increased with a peak value of 1. However, no striking improvement was observed in the residual NH_4^+–N removal as the Mg^{2+} dosage increased. In Nelson et al. [16], struvite precipitation decreased PO_4–P concentration by 85% at pH 9 for an initial Mg:P ratio of 1.2:1. In Wilsenach et al. [13], the phosphate removal was linear with an increasing Mg:P ratio, and 99% removal was achieved when the $MgCl_2$:P ratio was 1:1. Similar results were obtained in this study for low-strength ammonia conditions.

3.2.2. Response surface optimization study

According to the CCD, 20 groups of NH_4^+–N removal efficiency performance test experiments were designed (Table 3). The regression model was established by RSM, and the variance analysis and significance test of the regression equation was carried out. The results showed that the *F*-values of the regression models of NH_4^+–N removal efficiency was 125.97, and the *p*-value (Prob. > *F*) was less than 0.001, indicating that the CCD optimization method was

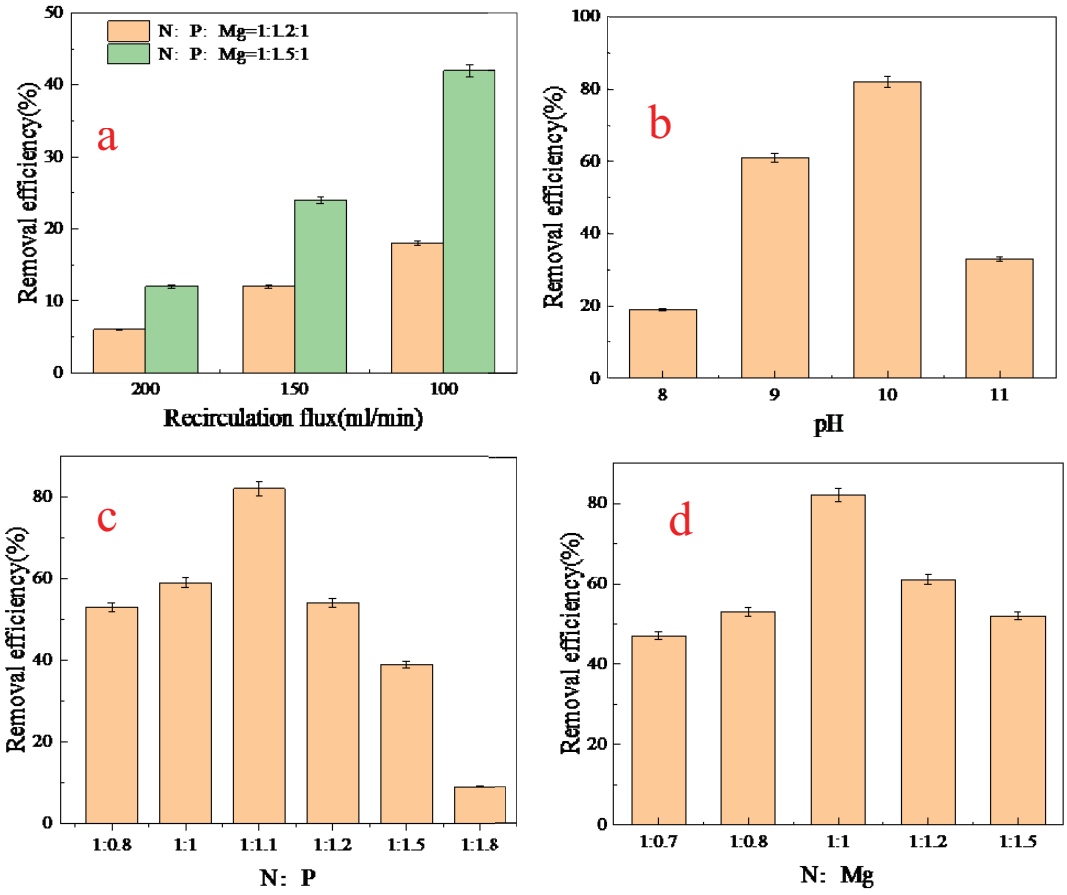

Fig. 3. Effects on NH_4^+ (30 mg/L) removal efficiency. (a) Recirculation flux, (b) pH (N:P:Mg = 1:1.1:1, recirculation flux of 100 mL/min), (c) N:P (pH = 10, recirculation flux of 100 mL/min), and (d) N:Mg (pH = 10, recirculation flux of 100 mL/min).

reliable and the variables had a significant influence on the response value, and the model was statistically significant. In addition, the fitting coefficients (R^2) of the model are 0.9913, which further indicates that the model has a high fitting degree between the predicted value and the measured value. The correction determination coefficient (Adj-R^2) was 0.9834, which could explain more than 98% of the data variability. So, the regression model can be used to accurately analyze the results.

As Fig. 4 shows, there were color changes and a contour map. The change in the color of the graph from green to red indicates the change of the extraction quality from less to more. The faster the change is, the greater the slope is, which means the more significant the impact on the experimental results. The response surface contour line can reflect the influence of various factors on the response value, and the minimum ellipse center in the contour line is the best advantage of the response value. The shape of the contour line can also reflect the strength of the interaction. The circle indicates that the interaction between the two factors is not significant, while the ellipse is the opposite. So, Fig. 4 shows that there was some interaction of pH, P:N, and Mg:N in contour map, and the color change shows the effects of pH and P:N was more significant than the effect of Mg:N. Table 3 shows the interaction of Fig. 4 in detail by data.

According to the RSM model, the pH was 10, P:N was 1.1:1, and Mg:N was 1:1 were suggested, and under this condition, the predicted optimal NH_4^+–N removal efficiency was 82.3%.

The influence of single factor on NH_4^+–N removal efficiency (%) was shown in Table 4. The sequence of the three factors was pH > P:N > Mg:N. The effects of pH (p = 0.0005) and P:N (p = 0.0023) were more significant than the effect of Mg:N (p = 0.0624). Table 4 also shows that the interaction of pH and Mg:N was significant [P = 0.0025 (p < 0.05)]; the interaction of pH and P:N was significant [P = 0.0234 (p < 0.05)]; and the interaction of Mg:N and P:N was not significant [P = 0.2109 (p > 0.05)].

On the basis of the performance data obtained from the present application, experimental results were compared with those of other studies in terms of the effects of various molar ratios on NH_4^+–N removal. In order to make a comparative evaluation of our data, ammonia nitrogen removal tests were conducted at similar experimental conditions (low-concentration ammonia nitrogen), using simulated wastewater. The performance of the present application was compared with other experimental data reported in the previous literature. In Yetilmezsoy and Sapci-Zengin [27], when the initial NH_4^+–N was 1,318 mg/L and the N:P:Mg ratio was 1:1:1, the NH_4^+–N removal efficiency was 85%. Ryu

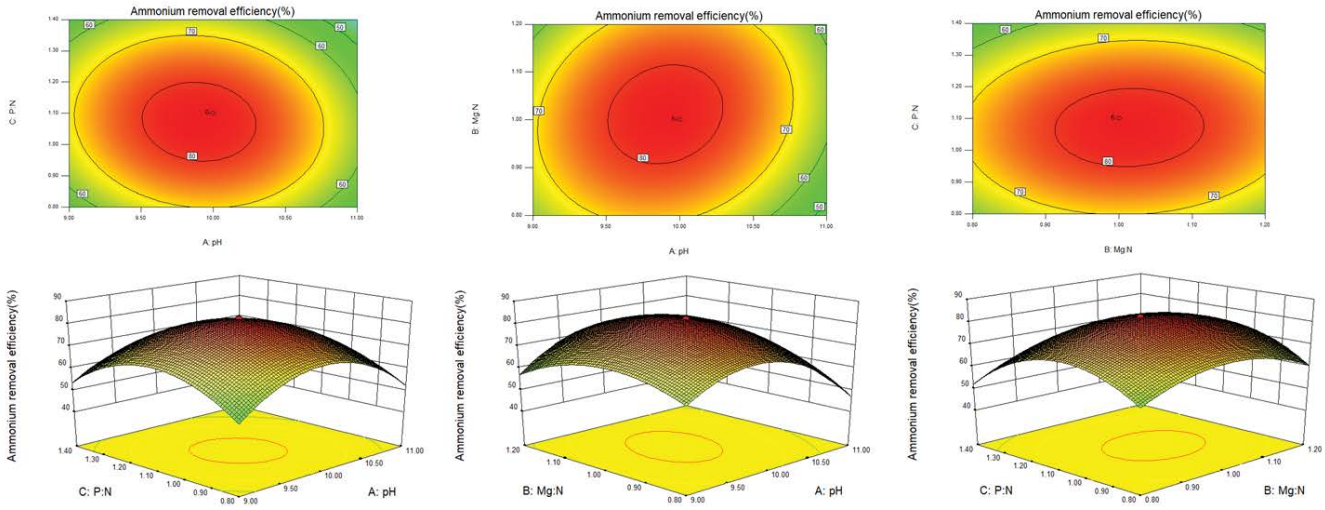

Fig. 4. Response surface plots showing the NH_4^+–N removal efficiency (%) with variable parameters pH, P:N, and Mg:N.

Table 3
Experimental design and the corresponding results

Number	Factor			Response
	pH	P:N	Mg:N	
1	10.00	1.00	1.10	82.4
2	9.00	0.80	0.80	49.9
3	11.00	1.20	0.80	45.0
4	9.00	0.80	1.40	48.0
5	11.68	1.00	1.10	28.0
6	8.32	1.00	1.10	38.0
7	10.00	1.00	1.10	82.5
8	10.00	1.00	1.10	82.4
9	9.00	1.20	0.80	42.9
10	10.00	1.00	1.60	35.0
11	9.00	1.20	1.40	41.0
12	10.00	1.34	1.10	59.0
13	11.00	1.20	1.40	37.9
14	11.00	0.80	0.80	42.0
15	11.00	0.80	1.40	25.0
16	10.00	0.66	1.10	48.0
17	10.00	1.00	1.10	82.3
18	10.00	1.00	1.10	82.2
19	10.00	1.00	0.60	42.0
20	10.00	1.00	1.10	82.6

et al. [38], when the initial NH_4^+–N was 143.5 mg/L and the N:P:Mg ratio was 1:1:1.2, the NH_4^+–N removal efficiency was 78%. In this study, when the initial NH_4^+–N was only 30 mg/L and the N:P:Mg ratio was 1:1.1:1, the NH_4^+–N removal efficiency was 82.3%. The comparison of results shows that the present results are close or superior to those reported by others. However, it was noted that the differences were probably due to the characteristics of the wastewaters that were studied as well as other operating conditions, such as

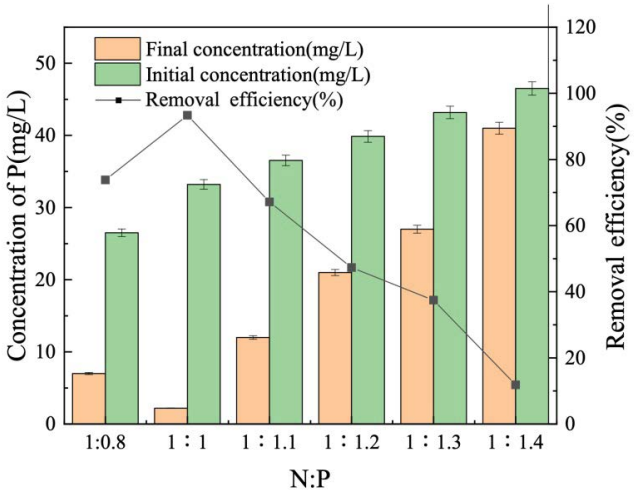

Fig. 5. Effect of N:P on phosphorus removal efficiency.

total mixing time, types of phosphate sources, and ions in the wastewater.

3.3. Phosphorus removal efficiency

Phosphorus removal efficiency should also be taken into consideration in actual wastewater treatment [40,41]. Low doses of PO_4^{3-} can lead to a decrease of residual PO_4^{3-} concentration (the residual PO_4^{3-} concentrations were 7.73 and 1.28 mg/L when the N:P ratios were 1:1 and 1:0.8). It was also reported by Uysal et al. [37] that as the N:P decreased the residual PO_4^{3-} also decreased. In Martí et al. [42], at an N:P ratio of 1:1, the ammonia removal ratio reached the maximum of approximately 83%, with a residual concentration of PO_4–P of 10 mg/L (removal efficiency was over 90%), and when N:P increased from 1:1.1 to 1:1.2, the removal efficiency decreased. Therefore, when the N:P ratios were 1:1.1 and 1:1, the removal efficiency of NH_4–N and phosphorus, respectively, reached their peaks (Fig. 5). This tendency was

Table 4
Significance test for regression coefficients

Source	Sum of squares	Degree of freedom	Mean square	*F*-value	*P*-value
Model	7,930.869	9	881.21	125.97	<0.0001
A-pH	174.51	1	174.51	24.95	0.0005
B-Mg:N	30.77	1	30.77	4.40	0.0624
C-P:N	115.83	1	115.83	16.56	0.0023
AB	112.50	1	112.50	16.08	0.0025
AC	50.00	1	50.00	7.15	0.0234
BC	12.50	1	12.50	1.79	0.2109
A^2	4,154.72	1	4,154.72	593.94	<0.0001
B^2	1,364.76	1	1,364.76	195.10	<0.0001
C^2	3,257.58	1	3,257.58	465.69	<0.0001

also confirmed by other studies. If ammonium removal is desired besides phosphorus, supplementary phosphorus is required, as reported by Münch and Barr [43], Ryu et al. [38], Stefanowicz et al. [44], and He et al. [45]. The effect of increasing concentrations of phosphorus on struvite precipitation has been investigated by many studies [46,47]. In addition, in their studies, for optimized results, the removal efficiency of NH_4–N was lower than that of phosphorus.

3.4. Characterization of struvite precipitation

Struvite crystal achieved under various conditions (molar ratio and pH) was characterized. As shown in Fig. 6a, a typical structure of needle-shaped crystallines with a smooth surface was observed for struvite obtained at pH 10, which matched previous research [48]. The crystals became smaller when the pH increased to 11, because the high pH induced higher nucleation density. Matynia [49] reported that when the pH increased from 9 to 11, the average size of the crystals decreased from 20.2 to 9.2 μm.

The molar ratio of P:Mg also plays an important role during struvite formation. As shown in Fig. 6, the increase of P:N:Mg changed the morphology of the precipitates. When the P:Mg ratio was 1:1.1, the crystals were needle-shaped. As the ratio increased to 1:1.5, the precipitates were mainly loose, cotton-shaped substances. The larger precipitates seem

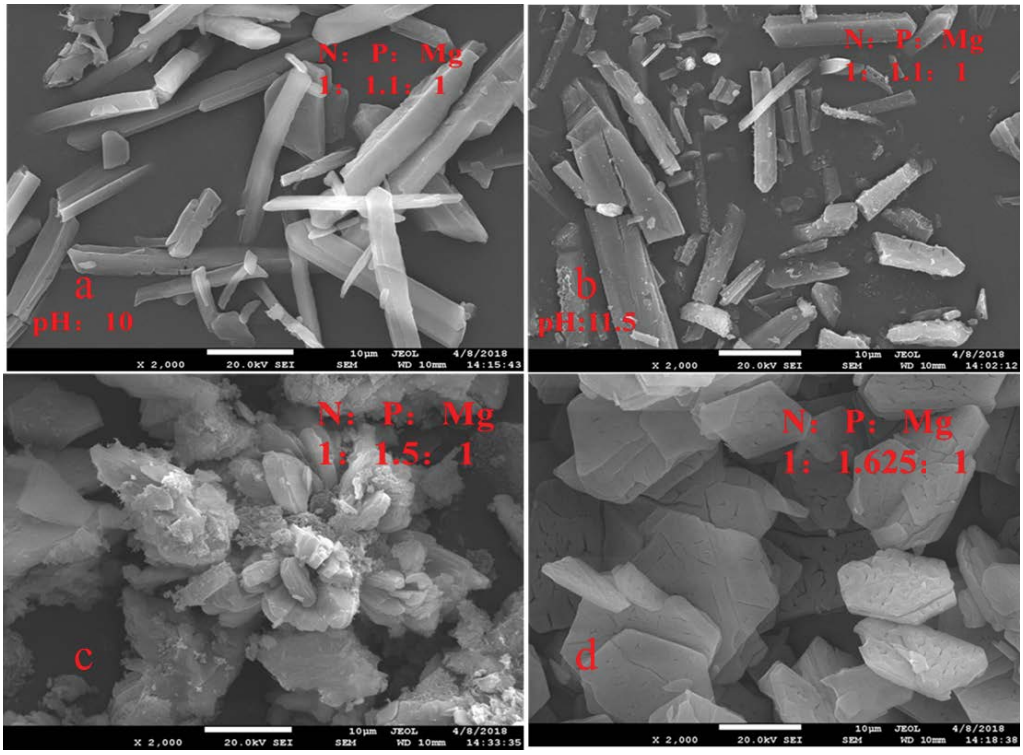

Fig. 6. Photograph of the crystals obtained in different N:P:Mg ratios.

to be needle-shaped struvite crystals covered with amorphous precipitates. When the ratio increased to 1:1.625, the precipitates began to form tabular crystals.

The struvite deposits of Figs. 6a and d were analyzed by XRD as shown in Fig. 7. It was exhibited that the samples extracted under the operating condition of N:P:Mg = 1:1.1:1 contained struvite. In comparison, samples of N:P:Mg = 1:1.625:1 contained both struvite and $Mg_3(PO_4)_2{\cdot}22H_2O$, which was consistent with the SEM morphologies.

The effect of atmospheric CO_2 dissolution on precipitate formation should also be considered, especially for open systems such as FBR in this study. Zhu found that atmospheric CO_2 had a major effect on the composition of the precipitates at pH higher than 9 during ammonia nitrogen removal from acetylene purification wastewater [50,51]. To evaluate the effects in the optimal conditions we obtained, Visual MINTEQ 3.1 was used to calculate the composition of precipitates at different equilibrium pH values for closed and partially open systems, which was assumed with a 20% atmospheric equilibrium. As shown in Figs. 8a and b, it seems that CO_2 dissolution did not have much effect on the systems, probably because of the relatively low concentrations of ammonia nitrogen and phosphate in the low-strength wastewater investigated in this study. For both systems, at pH of 8 and 8.5, the saturation index turned positive for struvite and $Mg_3(PO_4)_2$, and at optimal pH of 10, the saturation index was positive for struvite and $Mg_3(PO_4)_2$, indicating the potential of precipitation for both struvite and $Mg_3(PO_4)_2$, which was consistent with the XRD results.

4. Conclusion

Induced struvite crystallization in the FBR demonstrated its potential for ammonia recovery from low-strength ammonium wastewater treatment. Induced crystallization promoted struvite precipitation in low concentrations. It was demonstrated by RSM experiments that when the pH was 10, P:N was 1.1:1, and Mg:N was 1:1, the optimal NH_4^+–N removal efficiency was 82% for 30 mg/L N wastewater. The sequence of the influence of the three single factors on NH_4^+–N removal efficiency (%) was pH > P:N > Mg:N.

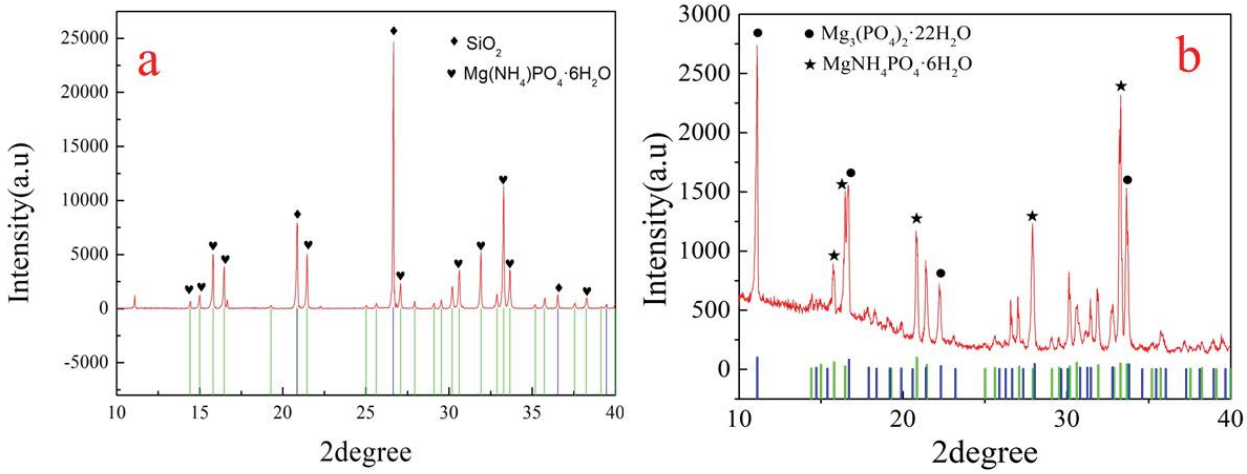

Fig. 7. XRD analysis for the solids formed (a) struvite pattern and (b) phosphate pattern.

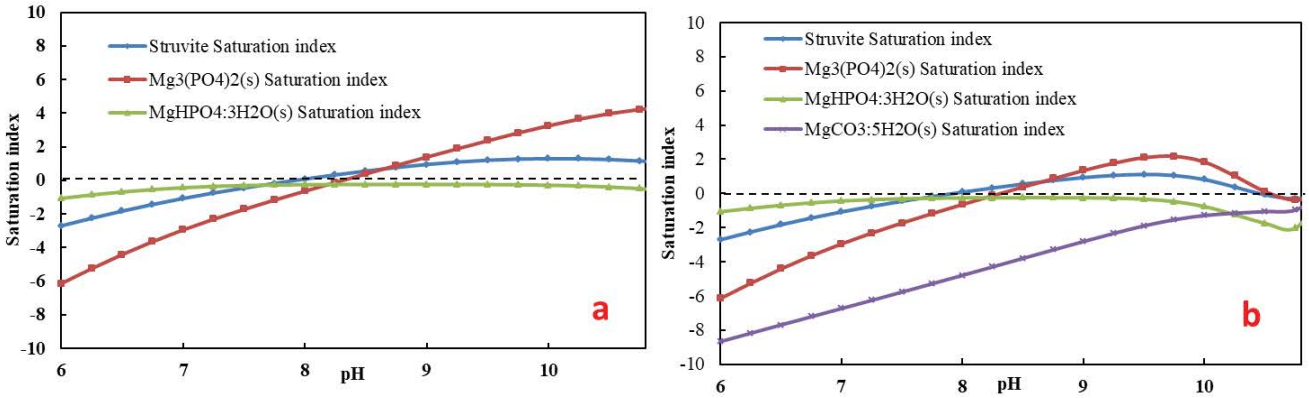

Fig. 8. Saturation index of model-predicted precipitate composition as a function of equilibrium pH under optimal conditions. Simulation conditions for Visual MINTEQ: ammonia nitrogen concentration = 2.14 mmol/L; phosphate concentration = 2.36 mmol/L; magnesium concentration = 2.14 mmol/L. (a) Closed system without atmospheric CO_2 and (b) partially open system equilibrium with 20% atmospheric CO_2 (pCO_2 = 0.000076 atm).

The main crystal achieved under optimal conditions was struvite, while the increase of P:N molar ratios (from 1 to 1.6) transformed some crystals from struvite to $Mg_2(PO_4)_2 \cdot 22H_2O$.

Acknowledgment

This work was supported by the Major Science and Technology Program for Water Pollution Control and Treatment of China (2017ZX07102-003, 2017ZX07103-003).

References

[1] L. Guo, Doing battle with the green monster of Taihu Lake, Science, 317 (2007) 1166–1166.
[2] National Environmental Protection Bureau, State Technology Supervision Bureau, Discharge Standard of Pollutants for Municipal Wastewater Treatment Plant, China Environmental Science Press, Peking, 2003.
[3] A. Pollice, V. Tandoi, C. Lestingi, Influence of aeration and sludge retention time on ammonium oxidation to nitrite and nitrate, Water Res., 36 (2002) 2541–2546.
[4] P.L. McCarty, J. Bae, J. Kim, Domestic wastewater treatment as a net energy producer–can this be achieved, Environ. Sci. Technol., 45 (2011) 7100–7106.
[5] H. Gong, Z. Jin, H. Xu, Q. Wang, J. Zuo, J. Wu, K. Wang, Redesigning C and N mass flows for energy-neutral wastewater treatment by coagulation adsorption enhanced membrane (CAEM)-based pre-concentration process, Chem. Eng. J., 342 (2018) 304–309.
[6] Z. Wang, H. Gong, Y. Zhang, P. Liang, K. Wang, Nitrogen recovery from low-strength wastewater by combined membrane capacitive deionization (MCDI) and ion exchange (IE) process, Chem. Eng. J., 316 (2017) 1–6.
[7] K. Fang, H. Gong, W. He, F. Peng, C. He, K. Wang, Recovering ammonia from municipal wastewater by flow-electrode capacitive deionization, Chem. Eng. J., 348 (2018) 301–309.
[8] B.E. Logan, Ending our hydrogen and ammonia addiction to fossil fuels, Environ. Sci. Technol., 6 (2019) 257–258.
[9] Y.H. Liu, J.H. Kwag, J.H. Kim, C.S. Ra, Recovery of nitrogen and phosphorus by struvite crystallization from swine wastewater, Desalination, 277 (2011) 364–369.
[10] Y. Ye, H.H. Ngo, W. Guo, Y. Liu, S.W. Chang, D.D. Nguyen, H. Liang, J. Wang, A critical review on ammonium recovery from wastewater for sustainable wastewater management, Bioresour. Technol., 268 (2018) 749–758.
[11] J.E. Lee, M.M. Rahman, C.S. Ra, Dose effects of Mg and PO_4 sources on the composting of swine manure, J. Hazard. Mater., 169 (2009) 801.
[12] S. Zhou, Y. Wu, Improving the prediction of ammonium nitrogen removal through struvite precipitation, Environ. Sci. Pollut., 19 (2012) 347–360.
[13] J.A. Wilsenach, C.A.H. Schuurbiers, M.C.M.V. Loosdrecht, Phosphate and potassium recovery from source separated urine through struvite precipitation, Water Res., 41 (2007) 458–466.
[14] S.P. Wei, F. van Rossum, G.J. van de Pol, M.-K.H. Winkler, Recovery of phosphorus and nitrogen from human urine by struvite precipitation, air stripping and acid scrubbing: a pilot study, Chemosphere, 212 (2018) 1030–1037.
[15] R.D. Schuiling, A. Andrade, Recovery of struvite from calf manure, Environ. Technol., 20 (1999) 765–768.
[16] N.O. Nelson, R.L. Mikkelsen, D.L. Hesterberg, Struvite precipitation in anaerobic swine lagoon liquid: effect of pH and Mg:P ratio and determination of rate constant, Bioresour. Technol., 89 (2003) 229.
[17] G.E. Diwani, S.E. Rafie, N.N.E. Ibiari, H.I. El-Aila, Recovery of ammonia nitrogen from industrial wastewater treatment as struvite slow releasing fertilizer, Desalination, 214 (2007) 200–214.
[18] Q. Ping, Y. Li, X. Wu, L. Yang, L. Wang, Characterization of morphology and component of struvite pellets crystallized from sludge dewatering liquor: effects of total suspended solid and phosphate concentrations, J. Hazard. Mater., 310 (2016) 261–269.
[19] D. Kim, H.D. Ryu, M.S. Kim, J. Kim, S.I. Lee, Enhancing struvite precipitation potential for ammonia nitrogen removal in municipal landfill leachate, J. Hazard. Mater., 146 (2007) 81–85.
[20] S. Uludag-Demirer, G.N. Demirer, S. Chen, Ammonia removal from anaerobically digested dairy manure by struvite precipitation, Process Biochem., 40 (2005) 3667–3674.
[21] Warmadewanthi, J.C. Liu, Recovery of phosphate and ammonium as struvite from semiconductor wastewater, Sep. Purif. Technol., 64 (2009) 368–373.
[22] Y.-J. Shih, R.R.M. Abarca, M.D.G. de Luna, Y.-H. Huang, M.-C. Lu, Recovery of phosphorus from synthetic wastewaters by struvite crystallization in a fluidized-bed reactor: effects of pH, phosphate concentration and coexisting ions, Chemosphere, 173 (2017) 466–473.
[23] Y.H. Song, G.L. Qiu, P. Yuan, X.Y. Cui, J.F. Peng, P. Zeng, L. Duan, L.C. Xiang, F. Qian, Nutrients removal and recovery from anaerobically digested swine wastewater by struvite crystallization without chemical additions, J. Hazard. Mater., 190 (2011) 140–149.
[24] J. Prywer, A. Torzewska, Bacterially induced struvite growth from synthetic urine: experimental and theoretical characterization of crystal morphology, Cryst. Growth Des., 9 (2009) 3538–3543.
[25] Z. Wei, Y. Xiong, J. Chen, J. Bai, J. Wu, J. Zuo, K. Wang, Recovery of Cu(II) from aqueous solution by induced crystallization in a long-term operation, J. Environ. Sci., 69 (2018) 183–191.
[26] H. Gong, Z. Wang, X. Zhang, Z. Jin, C. Wang, L. Zhang, K. Wang, Organics and nitrogen recovery from sewage via membrane-based pre-concentration combined with ion exchange process, Chem. Eng. J., 311 (2017) 13–19.
[27] K. Yetilmezsoy, Z. Sapci-Zengin, Recovery of ammonium nitrogen from the effluent of UASB treating poultry manure wastewater by MAP precipitation as a slow release fertilizer, J. Hazard. Mater., 166 (2009) 260–269.
[28] J.R. Burns, B. Finlayson, Solubility product of magnesium ammonium phosphate hexahydrate at various temperatures, J. Urol., 128 (1982) 426–428.
[29] A. Adnan, M. Dastur, D.S. Mavinic, F.A. Koch, Preliminary investigation into factors affecting controlled struvite crystallization at the bench scale, J. Environ. Eng. Sci., 3 (2004) 195–202.
[30] M.C.V.D. Leeden, D. Kashchiev, G.M.V. Rosmalen, Effect of additives on nucleation rate, crystal growth rate and induction time in precipitation, J. Cryst. Growth, 130 (1993) 221–232.
[31] N.C. Bouropoulos, P.G. Koutsoukos, Spontaneous precipitation of struvite from aqueous solutions, J. Cryst. Growth, 213 (2000) 381–388.
[32] Y. Song, P. Yuan, B. Zheng, J. Peng, F. Yuan, Y. Gao, Nutrients removal and recovery by crystallization of magnesium ammonium phosphate from synthetic swine wastewater, Chemosphere, 69 (2007) 319–324.
[33] H. Huang, J. Yang, D. Li, Recovery and removal of ammonia-nitrogen and phosphate from swine wastewater by internal recycling of struvite chlorination product, Bioresour. Technol., 172 (2014) 253.
[34] W. Li, X. Ding, M. Liu, Y. Guo, L. Liu, Optimization of process parameters for mature landfill leachate pretreatment using MAP precipitation, Front. Environ. Sci. Eng., 6 (2012) 892–900.
[35] M. Ronteltap, M. Maurer, R. Hausherr, W. Gujer, Struvite precipitation from urine- influencing factors on particle size, Water Res., 44 (2010) 2038–2046.
[36] J.D. Doyle, S.A. Parsons, Struvite formation, control and recovery, Water Res., 36 (2002) 3925.
[37] A. Uysal, Y.D. Yilmazel, G.N. Demirer, The determination of fertilizer quality of the formed struvite from effluent of a sewage sludge anaerobic digester, J. Hazard. Mater., 181 (2010) 248.
[38] H.D. Ryu, D. Kim, S.I. Lee, Application of struvite precipitation in treating ammonium nitrogen from semiconductor wastewater, J. Hazard. Mater., 156 (2008) 163–169.

[39] W. Song, Z. Li, F. Liu, Y. Ding, P. Qi, H. You, C. Jin, Effective removal of ammonia nitrogen from waste seawater using crystal seed enhanced struvite precipitation technology with response surface methodology for process optimization, Environ. Sci. Pollut. Res. Int., 25 (2018) 628–638.
[40] P. Battistoni, P. Pavan, M. Prisciandaro, F. Cecchi, Struvite crystallization: a feasible and reliable way to fix phosphorus in anaerobic supernatants, Water Res., 34 (2000) 3033–3041.
[41] E. Valsamijones, Phosphorus recovery from wastewater by struvite crystallization: a review, Crit. Rev. Env. Sci. Technol., 39 (2009) 433–477.
[42] N. Martí, L. Pastor, A. Bouzas, J. Ferrer, A. Seco, Phosphorus recovery by struvite crystallization in WWTPs: influence of the sludge treatment line operation, Water Res., 44 (2010) 2371–2379.
[43] E.V. Münch, K. Barr, Controlled struvite crystallisation for removing phosphorus from anaerobic digester sidestreams, Water Res., 35 (2001) 151–159.
[44] T. Stefanowicz, S. Napieralska-Zagozda, M. Osińska, K. Samsonowska, Ammonium removal from waste solutions by precipitation of $MgNH_4$ PO_4 II, Ammonium removal and recovery with recycling of regenerate, Resour. Conserv. Recycl., 6 (1992) 339–345.
[45] S. He, Y. Zhang, M. Yang, W. Du, H. Harada, Repeated use of MAP decomposition residues for the removal of high ammonium concentration from landfill leachate, Chemosphere, 66 (2007) 2233–2238.
[46] S.U.-Demirer, A study on nutrient removal from municipal wastewater by struvite formation using Taguchi's design of experiments, Environ. Eng. Sci., 25 (2008) 1–10.
[47] M. Türker, I. Celen, Removal of ammonia as struvite from anaerobic digester effluents and recycling of magnesium and phosphate, Bioresour. Technol., 98 (2007) 1529–1534.
[48] A. Korchef, H. Saidou, A.M. Ben, Phosphate recovery through struvite precipitation by CO_2 removal: effect of magnesium, phosphate and ammonium concentrations, J. Hazard. Mater., 186 (2011) 602–613.
[49] A. Matynia, B. Wierzbowska, N. Hutnik, K. Piotrowski, R. Liszka, T. Ciesielski, A. Mazienczuk, Method for struvite recovery from a wastewater of mineral fertilizer industry, Przem. Chem., 89 (2010) 478–485.
[50] L. Zhu, D.M. Dong, X.Y. Hua, Z.Y. Guo, D.P. Liang, Ammonia nitrogen removal from acetylene purification wastewater from a PVC plant by struvite precipitation, Water Sci. Technol., 74 (2016) 508–515.
[51] L. Zhu, D.M. Dong, X.Y. Hua, Y. Xu, Z.Y. Guo, D.P. Liang, Ammonia nitrogen removal and recovery from acetylene purification wastewater by air stripping, Water Sci. Technol., 75 (2017) 2538–2545.